Celastrol ameliorates experimental autoimmune neuritis by shifting the polarization of M1/M2 macrophages via the hypoxic response pathway

Yun Qian (qqyyqqyy@163.com)
Affiliated Hangzhou First People's Hospital,Zhejiang University School of Medicine
https://orcid.org/0000-0002-4413-7813
Bo Tang
Hangzhou First People's Hospital
Minhai Jiang
Hangzhou First People's Hospital
Shan Lu
Hangzhou First People's Hospital
Huan Huang
Hangzhou First People's Hospital
Wan Wei
Hangzhou First People's Hospital

Research

Keywords: celastrol, experimental autoimmune neuritis, macrophage polarization, hypoxia response

Posted Date: May 8th, 2020

DOI: https://doi.org/10.21203/rs.3.rs-25002/v1

Abstract

Background

GBS is an autoimmune disease characterized by inflammatory infiltration and demyelination of peripheral nerves. Macrophage polarization is involved in different stages of GBS. Altering the polarization of macrophages may be an effective therapeutic strategy for GBS. Celastrol was previously shown to contribute to anti-neuroinflammation. However, the mechanism underlying the effect of celastrol in GBS animal model experimental autoimmune neuritis (EAN) is unclear. We hypothesized that celastrol may shift the polarization of macrophages through the NRF /HIF-1αpathway.

Methods

Clinical scores, weight and histological changes were assessed to investigate the effects of celastrol on EAN. To detect the polarization state of macrophages, flow cytometry and immunofluorescence staining were applied. Inflammation cytokines were evaluated by ELISA. The expression of NRF2 and HIF-1α were detected by western-blot and immunofluorescence staining.

Results

Celastrol treatment significantly ameliorates the severity and neuroinflammation of EAN. The polarization state of macrophages from M1 to M2 was observed upon celastrol application. Consistently, pro-inflammatory cytokines were decreased, whereas anti-inflammatory cytokines were increased upon celastrol treatment. Furthermore, we found that celastrol treatment may increase expression of Nrf2 and decrease the expression of HIF-1α.

Conclusion

Taken together, these data demonstrate that celastrol may ameliorate the severity and neuroinflammation of EAN via promoting the polarization state of macrophages into M2, likely by modulating the hypoxic response. Celastrol may therefore serve as a novel therapeutic agent for GBS.

Background

Guillain Barre syndrome (GBS) is a spectrum of immune-mediated acute inflammatory peripheral neuropathies. Acute inflammatory demyelinating polyneuropathy (AIDP) is the most common subtype of GBS and is characterized by acute weakness of extremities and areflexia. Currently, intravenous immunoglobulin (IVIG) and plasma exchange are proven effective therapies for GBS(1). Although most patients survive, approximately 3% of GBS patients die and 20% suffer from severe disability after six months(2). Therefore, more efficacious treatments are needed.

Experimental autoimmune neuritis (EAN) is an animal model of AIDP that can mimic the clinical, histopathological, and immunological features of human AIDP(3, 4). Similar to AIDP, EAN is characterized

by accumulation of T cells and macrophages, breakdown of the blood-nerve barrier (BNB), and demyelination of peripheral nerves(2, 3). As the main infiltrating cells in the peripheral nervous system (PNS) during AIDP progression, macrophages play either a proinflammatory or an anti-inflammatory role at the different stages of AIDP(3, 5). Importantly, a shift in macrophage polarization from the M1 to M2 phenotype may ameliorate the severity of EAN and, thus, is suggestive of a promising therapeutic strategy for treating GBS(5–7).

In the past decade, some traditional Chinese medicines have been found to be effective for treating GBS(8, 9). These studies have highlighted the unique clinical efficacies of traditional medicine. However, the underlying cellular and molecular mechanisms of these medicines remain to be investigated. Celastrol is an active ingredient of the traditional Chinese medicine, *Tripterygium wilfordii* (Thunder god vine), which has long been used to treat inflammatory diseases. Together with artemisinin, a previous study reported the potential of celastrol as a clinical drug for the treatment of obesity, with other possible uses as well(10). Furthermore, experimental findings have indicated that celastrol can reduce inflammation by suppressing M1 polarization(11). During the polarization of macrophages, hypoxic adaptive responses are actively regulated(5, 6, 11). As a transcription factor with a high antioxidant capacity, nuclear factor-E2-related factor 2 (NRF2) exerts protective effects against oxidative and inflammatory stress by regulating antioxidant response elements (AREs) and heme oxygenase 1 (HO-1) (12, 13). Furthermore, hypoxia-inducible factor (HIF-1α), known as one of the most important mediators in cellular responses to hypoxia and inflammation, has been reported to contribute to shifting the polarization of macrophages(14, 15). However, the role of the NRF2 signaling pathway in regulating HIF-1α remains unclear. Herein, we hypothesized that celastrol may shift the polarization of macrophages via the hypoxia response pathway.

In the present study, we investigated the effects and mechanisms of celastrol in an EAN model of GBS. Our translational findings demonstrate that celastrol may be effective in ameliorating the clinical course of GBS by decreasing infiltration of inflammatory cells. Furthermore, our elucidated therapeutic effect of celastrol may be related to promoting macrophage polarization toward the anti-inflammatory phenotype via the hypoxia response pathway.

Materials And Methods

Animals

Male Lewis rats (6–8 weeks old, 160–180 g, Vital River, Beijing, China) were acclimated to the environment within our institution’s vivarium for one week prior to the start of any experiments. All rats were housed under equal daily periods of light and darkness (i.e., 12/12-h light/dark cycle) and were provided access to food and water *ad libitum*. The rats were randomly assigned to the following three groups: the control, EAN, and therapeutic (i.e., celastrol + EAN) groups (n = 8 per group). All efforts were made to minimize the numbers of animals used and their suffering. All animal experimental protocols

were reviewed and approved by the Animal Ethics Committee of Zhejiang University of Traditional Chinese Medicine.

Induction Of Ean And Celastrol Treatments

The inoculum preparation was as follows. The P2 peptides 53–78 (TGSPPLATGISPLLGGGPGGTTAAAA, GL, Biochem Ltd. Shanghai, China) were dissolved in phosphate-buffered saline (PBS; 2 mg/ml) and were then emulsified with an equal volume of complete Freund's adjuvant (CFA; Difco) containing *Mycobacterium tuberculosis* (strain H37RA). The final concentration of peptides in the inoculum was 1 mg/ml. EAN was induced by immunization via subcutaneous injection of 0.3 ml of inoculum to the base of the tail. For celastrol treatments, rats were induced by intragastric administration with celastrol at a dose of 1 mg/kg(16). Celastrol was prepared as a 0.2-mg/ml solution in 1% dimethyl sulfoxide (DMSO). Rats in both the control and EAN groups were given an equal volume of vehicle (i.e., 1% DMSO).

Body weights and neurological scores were recorded every day. Neurological signs were assessed by two investigators, blind to the designations of rats among the experimental groups, as follows: normal (score = 0); reduced tonus of tail (score = 1); impaired righting and limp tail (score = 2); absent righting (score = 3) and gait ataxia (score = 4); mild paresis of the hind limbs (score = 5); moderate paraparesis (score = 6); severe paraparesis or paraplegia of the hind limbs (score = 7); tetraparesis (score = 8); moribund (score = 9); and death (score = 10)(6, 9).

Histopathological Assessments

To evaluate the infiltration of inflammatory cells and demyelination in the PNS, hematoxylin-eosin (HE) and Luxol fast blue (LFB) were applied to peripheral tissues. Specifically, sciatic nerves were harvested at the peak of disease (day-16 post-immunization [p.i.]) and immediately fixed in 4% paraformaldehyde overnight at 4 °C. After dehydration and vitrification, the harvested sciatic nerves were embedded in paraffin and sliced into 4-um-thick sections. The sciatic-nerve sections were then stained with HE and LFB. The infiltration of inflammatory cells was counted at a 200-x magnification from five fields randomly from each slide. The averaged results are expressed as the number of inflammatory cells per square millimeter. Histological scores were applied to evaluate the severity of demyelination according to a semiquantitative grading system, as follows[20]: 0 = normal; 1 = less than 25% demyelinated fibers; 2 = 25–50% demyelinated fibers; 3 = 50–75% demyelinated fibers; and 4 = more than 75% demyelinated fibers.

Immunofluorescence was performed according to the protocols provided by the manufacturers from which the employed antibodies were purchased. First, 4-um-thick sections were permeabilized in 0.3% Triton X100. After blocking the tissues, sections were incubated with the following primary antibodies at 4 °C overnight: mouse anti-CD68 (1:200, Abcam); rabbit anti-iNOS (1:200, Abcam); rabbit anti-CD163 (1:200, Abcam); mouse anti-NRF2 (1:100, Abcam); and rabbit anti-HIF-1α (1:100, Abcam). The next day,

sections were washed in PBS and incubated with the following specific fluorochrome-conjugated secondary antibodies: Alexa Fluor 555 conjugated goat anti-mouse IgG (H + L) (1:200, Thermo Fisher); Alexa Fluor 488 conjugated goat anti-rabbit IgG (H + L) (1:200, Thermo Fisher); Alexa Fluor 488 conjugated goat anti-mouse IgG (H + L) (1:100, Life Technologies); and Alexa Fluor 555 conjugated goat anti-rabbit IgG (H + L) (1:100, Life Technologies). Finally, sections were stained with 4',6-diamidino-2-phenylindole (DAPI) to label cellular nuclei. Images were acquired using an 20 × objective with an Olympus microscope. Image-Pro Plus was applied to quantify the fluorescent intensity of each image.

Western Blotting

Lysis buffer was used to extract protein from sciatic-nerve tissues. The bicinchoninic acid (BCA) protein method was used to measure protein concentrations. Samples (20 ug each) were loaded on 10% sodium dodecyl sulfate (SDS)-polyacrylamide gel electrophoresis (PAGE) gels and were then electrophoretically separated. Proteins were then transferred to polyvinylidene difluoride (PVDF) membranes. After blocking, membranes were then incubated overnight at 4 °C with primary antibodies against the following: NRF2 (1:1000, Abcam), HIF-1α (1:1000, Abcam), and GAPDH (1:5000, Multi Science). The next day, the membranes were washed with Tris-buffered saline with Tween (TBST) and were subsequently incubated with secondary antibodies—goat anti-mouse IgG (1:5000, Multi Science) and goat anti-rabbit IgG (1:5000, Multi Science)—for 2 h at room temperature. After washing the membranes, chemiluminescence reactions were carried out and immunoreactivity levels were detected by a gel imaging analyzer (Bio-Rad).

Flow Cytometry

Splenocytes were harvested under sterile conditions at the peak of disease (day-16 p.i.). After fixation and permeabilization, splenocytes were incubated with antibodies for intracellular iNOS (1:50, Abcam) and rabbit anti-rat CD163 (1:50, Abcam) overnight at 4 °C. Subsequently, fixed cells were then labelled with AlexaFluor 647 and AlexaFluor 700, after which splenocytes were stained with fluorescein isothiocyanate (FITC)-conjugated mouse anti-rat CD68 (1:500, Thermo Fisher) for 30 min at 4 °C. The data were acquired using an Accuri C6 flow cytometer (BD Biosciences) and were analyzed via FlowJo software.

Enzyme-linked Immunosorbent Assays (elisas)

Sera and spleens were collected at the peak of disease (day-16 p.i.). To analyze the levels of cytokines—including interleukin 4 (IL-4), IL-6, IL-10, and tumor necrosis factor (TNF-α)—specific enzyme-linked immunosorbent assay (ELISA) kits (Multi Science) were used following the manufacturer's instructions, as previously described. The concentrations of IL-4, IL-6, IL-10, and TNF-α were compared to standard curves.

Statistical analysis

All data are presented as the mean ± standard deviation (SD). GraphPad Prism 8 was used to analyze the data. Mann-Whitney U tests were used to compare differences of neurologic scores and histological scores among the experimental groups. Student's t-tests and one-way or two-way analyses of variance (ANOVAs) were applied for paired and multiple group comparisons. Statistical significance was set at a level of $p < 0.05$.

Results

Celastrol ameliorates the severity of EAN

To investigate the effect of celastrol in EAN, rats were treated with celastrol (1 mg/kg) daily from the day of EAN immunization. Neurological scores (Fig. 1A) were recorded every day and weight changes were recorded every three days (Fig. 1B). The EAN group of rats started to exhibit neurological symptoms on day-6 p.i., and the symptoms progressed rapidly until they peaked on day-16 p.i.. (mean pathological score, 6.80 ± 0.45) (Fig. 1C). Compared to parameters in the EAN group, the celastrol treatment group exhibited a delayed onset of neuritis, decreased mean peak neurological scores, and lower neurological scores from days 8 to 16 p.i. ($p < 0.05$ for each time point) (Fig. 1A). Moreover, compared to those of the control group, the mean body-weight trends of rats were decreased in the EAN group while this decrease occurred more slowly in the EAN + celastrol group relative to that of the EAN group (Fig. 1B, D). These results demonstrated that celastrol treatments not only delayed the onset of EAN but also ameliorated the severity of EAN symptoms.

Celastrol attenuates the histopathology and infiltration of inflammatory cells in EAN

We next investigated the histopathology of the sciatic nerve at day-16 p.i. from each rat. Compared to that of the EAN group (518.08 ± 61.26 cells), we found that the number of infiltrating inflammatory cells was significantly reduced in the celastrol treatment group, as revealed by HE staining (282.86 ± 92.45 cells) ($p < 0.05$) (Fig. 2A, C). Furthermore, the incidence of demyelination was decreased in the celastrol group compared to that in the EAN group (Fig. 2B). The mean histological scores, which were used to semi-quantitatively evaluate the severity of demyelination, were markedly lower in the celastrol treatment group (1.67 ± 0.67) compared to those in the EAN group (2.89 ± 0.74, $p < 0.05$) in LFB staining (Fig. 2B, D).

Celastrol promotes polarization of macrophages to the M2 phenotype in EAN

We further investigated whether the therapeutic efficacy of celastrol correlated with polarization of macrophages within sciatic nerves and spleens of EAN rats. Immunofluorescent staining was used to evaluate the phenotypes of macrophages at day-16 p.i. in sciatic nerves. Compared to those in the control group, we found that the levels of infiltrating macrophages were elevated (Fig. 3A) in the EAN group, while the levels of both M1 and M2 macrophages were reduced (Fig. 3A) in the celastrol treatment group. Moreover, compared to that in EAN rats, the ratio of M2/M1 macrophages was significantly elevated in celastrol-treated rats (Fig. 3A). In addition, we also used flow cytometry to detect the polarization state of macrophages in spleens. The flow cytometry results showed a similar macrophage polarization (Fig. 3B). Compared to those in the EAN group, both results showed an increase in the percentages of M2 macrophages and a decrease in the percentages of M1 macrophages in the celastrol treatment group (Fig. 3B, C), indicating that celastrol promoted polarization of macrophages into the M2 phenotype in EAN.

Celastrol reduces inflammatory cytokines while boosting anti-inflammatory cytokines in EAN

We also examined whether the benefits of celastrol treatment were related to the expression profiles of inflammation cytokines. TNF-α, IL-6, IL-4, and IL-10 levels were evaluated in the sera and spleens collected on day-16 p.i. from control, EAN, and celastrol treatment rats. Compared to those in the control group, the levels of IL-6 and TNF-α in the EAN group were elevated (Fig. 4A, B), while the levels of IL-4 and IL-10 were reduced (Fig. 4C, D). By contrast, celastrol treatment significantly reduced IL-6 and TNF-α pro-inflammatory cytokine levels, whereas IL-4, and IL-10 anti-inflammatory cytokine levels were elevated on day-16 p.i. (Fig. 4).

Celastrol Regulates The Nrf2/hif-1α Hypoxic Pathway In Ean

To further elucidate whether the NRF2/HIF-1α pathway is related to the therapeutic effects of celastrol treatment, we analyzed NRF2 and HIF-1α expression levels in sciatic-nerve tissue via immunofluorescence and Western blotting. When compared to these levels in the control group, a decreased level of NRF2 and an increased level of HIF-1α were observed (Fig. 5A) in the EAN group, whereas the celastrol treatment group showed an increased level of NRF2 and a decreased level of HIF-1α on day-16 p.i. compared to those in the EAN group (Fig. 5A). Consistently, the results of Western blotting also showed an increased level of NRF2 and a decreased level of HIF-1α compared to those in the EAN group (Fig. 5B, C).

Discussion

In the present study, we assessed the effects of celastrol treatment on EAN, which is a widely applied animal model of GBS. We found that celastrol not only delayed the onset of EAN but also attenuated its peak severity. Histopathologically, we revealed that celastrol attenuated EAN-induced infiltration of inflammatory cells and demyelination of sciatic nerves (Fig. 6).

Celastrol, as an effective ingredient of *Tripterygium wilfordii* (Thunder god vine), has a long history in the treatment of inflammatory and autoimmune disease. Pharmacologically, celastrol exhibits anti-cancer, anti-inflammatory, and antioxidant properties(17–19). In inflammatory disease, celastrol had been found to ameliorate myelin oligodendrocyte glycoprotein (MOG)-induced EAE development by reducing Th17 responses in both the periphery and central nervous system (CNS)(20). Celastrol also switches T-cell responses from a predominantly Th1 to Th2 type(16). Moreover, celastrol may also reduce NF-κB expression and T-cell accumulation in the CNS, indicating its anti-inflammatory properties(20, 21). Based on these previous findings, we hypothesized that celastrol might have the potential to treat EAN. To our knowledge, the present study represents the first to investigate the effect of celastrol on EAN. Consistent with previous reports, we found that celastrol attenuated inflammatory reactions and demyelination in the PNS and improved EAN outcomes by reducing infiltration of inflammatory cells.

GBS comprises a spectrum of autoimmune disorders that induce peripheral neuropathies, during which the infiltration of inflammatory cells into the PNS occurs at different stages of the disease(2). As the major inflammatory cells in EAN, macrophages are generally divided into two phenotypes: classically activated (M1) and alternatively activated (M2) macrophages(22). Previous studies suggest that macrophage phenotypes have high plasticity and can be altered by appropriate signals at different stages of GBS(5, 23, 24). M1 macrophages play a pro-inflammatory role in tissue damage and disease progression, while M2 macrophages exert anti-inflammatory effects and promote disease recovery(3). In the present study, we observed that celastrol yielded a favorable outcome in EAN that was associated with a phenotypic switch toward M2 macrophages within sciatic nerves. Furthermore, splenic macrophages also showed a switch toward M2 macrophages during celastrol treatment in the face of EAN, indicating that celastrol may attenuate EAN through promoting polarization of macrophages into the M2 phenotype within multiple tissues.

Inflammatory cytokines secreted by macrophages mediate immune responses. M1 macrophages are involved in the progression of EAN by releasing pro-inflammatory cytokines such as TNF-α and IL-6 (25, 26). Previous studies have shown that TNF-α levels are elevated in EAN/GBS, leading to the disruption of the BNB and the demyelination of peripheral nerves(27, 28). Furthermore, IL-6 has been shown to contribute to the demyelination and progression of EAN, and increased IL-6 levels have been observed in EAN and in the sera and cerebrospinal fluid of GBS patients(26). In contrast, M2 macrophages exert a protective role by releasing anti-inflammatory cytokines, including IL-4 and IL-10(29–32). Importantly, anti-inflammatory cytokines have been previously found to be involved in the repair of peripheral nerves. In accordance with previous studies, we observed increased levels of TNF-α and IL-6 and decreased levels of IL-4 and IL-10 in both the spleen and peripheral venous blood in the EAN group. Although these particular protein levels may not fully represent all cytokine levels in peripheral nerves, they nonetheless

provide molecular clues as to the underling physiological mechanisms of celastrol, which are suggestive of a shift in the polarization of macrophages to the M2 phenotype to ameliorate EAN.

Hypoxia is a physiological state of the micro-environment that is involved in the development of many diseases. NRF2 is a transcription factor that plays a pivotal role in hypoxia (13, 33). Activation of NRF2 exerts antioxidant, anti-inflammatory, and neuroprotective properties(34, 35). Upregulation of NRF2 induces HO-1 gene transcription, which is implicated in ameliorating the severity of EAN rats(6). HIF-1α is another key transcription factor that responds to hypoxia. In obesity, HIF-1α activation is triggered by increased oxygen consumption, thus causing inflammation(10). Inhibition of HIF-1α may decrease inflammation in tumor genesis (36). Furthermore, growing evidence has suggested that NRF2 and HIF-1α can directly or indirectly regulate each other (37, 38). A recent study found that NRF2 may upregulate HIF-1α via activation of thioredoxin in stem cells (39). HIF-1α can elevate NRF2 by inhibiting thioredoxin reductase (40). However, these two factors do not always reinforce each other. During andrographolide treatment, a previous study showed that the expression level of NRF2 was increased while the HIF-1α level decreased (41). Interestingly, we observed that celastrol significantly increased the expression of NRF2 and decreased the expression of HIF-1α, indicating that celastrol may exert anti-inflammation and neuroprotective effects by modulating hypoxia.

Conclusion

In conclusion, the present study demonstrates that celastrol may ameliorate EAN progression through promoting polarization of macrophages into the M2 phenotype, possibly by modulating hypoxic responses. Hence, our findings suggest that celastrol may represent a potential novel therapy for GBS.

Abbreviations

GBS:Guillain-Barré syndrome; AIDP:acute inflammatory demyelinating polyneuropathy; IVIG:intravenous immunoglobulin; EAN:experimental autoimmune neuritis; BNB:blood-nerve barrier; PNS:peripheral nervous system; NRF2:nuclear factor-E2-related factor 2; AREs:antioxidant response elements; HO-1:heme oxygenase; HIF-1α:hypoxia-inducible factor 1α; DMSO:dimethyl sulfoxide; HE:hematoxylin-eosin; LFB:Luxol fast blue ; ELISA:Enzyme-linked immunosorbent assay; BCA:bicinchoninic acid; SDS:sodium dodecyl sulfate; PAGE:polyacrylamide gel electrophoresis; PVDF:polyvinylidene difluoride; TBST:Tris-buffered saline with Tween; IL-4:interleukin 4; TNF-α:tumor necrosis factor; MOG:myelin oligodendrocyte glycoprotein; CNS:central nervous system;

Declarations

Ethics Approval And Consent To Participate

All animal experimental protocols were reviewed and approved by the Animal Ethics Committee of Zhejiang University of Traditional Chinese Medicine.

Consent For Publication

Not applicable.

Availability of Data And Material

The datas are available from the corresponding author on reasonable request.

Competing interests

The authors declared that they have no competing interests.

Fundings

This work was financially supported by Zhejiang Science and Technology Program of traditional Chinese medicine (2019ZQ037), Medical Science and Technology Project of Zhejiang Province(2018KY584)

Authors' contributions

YQ carried out the general studies and drafted the manuscript. BT participated in the design of the study and performed the statistical analysis. MJ prepared the figures. SL,WW and HH performed the laboratory experiments. All authors read and approved the final manuscript.

Acknowledgements

Not applicable.

References

1. Jasti AK, Selmi C, Sarmiento-Monroy JC, Vega DA, Anaya JM, Gershwin ME. Guillain-Barre syndrome: causes, immunopathogenic mechanisms and treatment. Expert review of clinical immunology. 2016;12(11):1175-89.
2. Yuki N, Hartung HP. Guillain-Barre syndrome. The New England journal of medicine. 2012;366(24):2294-304.
3. Zhang HL, Zheng XY, Zhu J. Th1/Th2/Th17/Treg cytokines in Guillain-Barre syndrome and experimental autoimmune neuritis. Cytokine & growth factor reviews. 2013;24(5):443-53.
4. Zhu J, Mix E, Link H. Cytokine production and the pathogenesis of experimental autoimmune neuritis and Guillain-Barre syndrome. Journal of neuroimmunology. 1998;84(1):40-52.

5. Shen D, Chu F, Lang Y, Geng Y, Zheng X, Zhu J, et al. Beneficial or Harmful Role of Macrophages in Guillain-Barre Syndrome and Experimental Autoimmune Neuritis. Mediators of inflammation. 2018;2018:4286364.
6. Han R, Xiao J, Zhai H, Hao J. Dimethyl fumarate attenuates experimental autoimmune neuritis through the nuclear factor erythroid-derived 2-related factor 2/hemoxygenase-1 pathway by altering the balance of M1/M2 macrophages. Journal of neuroinflammation. 2016;13(1):97.
7. Jin T, Yu H, Wang D, Zhang H, Zhang B, Quezada HC, et al. Bowman-Birk inhibitor concentrate suppresses experimental autoimmune neuritis via shifting macrophages from M1 to M2 subtype. Immunology letters. 2016;171:15-25.
8. Lee HJ, Park IS, Lee JI, Kim JS. Guillain-Barre syndrome following bee venom acupuncture. Internal medicine (Tokyo, Japan). 2015;54(8):975-8.
9. Xu L, Li L, Zhang CY, Schluesener H, Zhang ZY. Natural Diterpenoid Oridonin Ameliorates Experimental Autoimmune Neuritis by Promoting Anti-inflammatory Macrophages Through Blocking Notch Pathway. Frontiers in neuroscience. 2019;13:272.
10. Liu J, Lee J, Salazar Hernandez MA, Mazitschek R, Ozcan U. Treatment of obesity with celastrol. Cell. 2015;161(5):999-1011.
11. Luo D, Guo Y, Cheng Y, Zhao J, Wang Y, Rong J. Natural product celastrol suppressed macrophage M1 polarization against inflammation in diet-induced obese mice via regulating Nrf2/HO-1, MAP kinase and NF-kappaB pathways. Aging. 2017;9(10):2069-82.
12. Bryan HK, Olayanju A, Goldring CE, Park BK. The Nrf2 cell defence pathway: Keap1-dependent and -independent mechanisms of regulation. Biochemical pharmacology. 2013;85(6):705-17.
13. Nguyen T, Nioi P, Pickett CB. The Nrf2-antioxidant response element signaling pathway and its activation by oxidative stress. The Journal of biological chemistry. 2009;284(20):13291-5.
14. Deng W, Feng X, Li X, Wang D, Sun L. Hypoxia-inducible factor 1 in autoimmune diseases. Cellular immunology. 2016;303:7-15.
15. Lee YS, Kim JW, Osborne O, Oh DY, Sasik R, Schenk S, et al. Increased adipocyte O2 consumption triggers HIF-1alpha, causing inflammation and insulin resistance in obesity. Cell. 2014;157(6):1339-52.
16. Abdin AA, Hasby EA. Modulatory effect of celastrol on Th1/Th2 cytokines profile, TLR2 and CD3+ T-lymphocyte expression in a relapsing-remitting model of multiple sclerosis in rats. European journal of pharmacology. 2014;742:102-12.
17. Venkatesha SH, Dudics S, Astry B, Moudgil KD. Control of autoimmune inflammation by celastrol, a natural triterpenoid. Pathogens and disease. 2016;74(6).
18. Xi J, Li Q, Luo X, Wang Y, Li J, Guo L, et al. Celastrol inhibits glucocorticoidinduced osteoporosis in rat via the PI3K/AKT and Wnt signaling pathways. Molecular medicine reports. 2018;18(5):4753-9.
19. Yang Y, Cheng S, Liang G, Honggang L, Wu H. Celastrol inhibits cancer metastasis by suppressing M2-like polarization of macrophages. Biochemical and biophysical research communications. 2018;503(2):414-9.

20. Wang Y, Cao L, Xu LM, Cao FF, Peng B, Zhang X, et al. Celastrol Ameliorates EAE Induction by Suppressing Pathogenic T Cell Responses in the Peripheral and Central Nervous Systems. Journal of neuroimmune pharmacology : the official journal of the Society on NeuroImmune Pharmacology. 2015;10(3):506-16.
21. Zhang X, Zhao W, Liu X, Huang Z, Shan R, Huang C. Celastrol ameliorates inflammatory pain and modulates HMGB1/NF-kappaB signaling pathway in dorsal root ganglion. Neuroscience letters. 2019;692:83-9.
22. Sica A, Mantovani A. Macrophage plasticity and polarization: in vivo veritas. The Journal of clinical investigation. 2012;122(3):787-95.
23. Davies LC, Jenkins SJ, Allen JE, Taylor PR. Tissue-resident macrophages. Nature immunology. 2013;14(10):986-95.
24. Muller J, von Bernstorff W, Heidecke CD, Schulze T. Differential S1P Receptor Profiles on M1- and M2-Polarized Macrophages Affect Macrophage Cytokine Production and Migration. BioMed research international. 2017;2017:7584621.
25. Ebrahim Soltani Z, Rahmani F, Rezaei N. Autoimmunity and cytokines in Guillain-Barre syndrome revisited: review of pathomechanisms with an eye on therapeutic options. European cytokine network. 2019;30(1):1-14.
26. Lu MO, Zhu J. The role of cytokines in Guillain-Barre syndrome. Journal of neurology. 2011;258(4):533-48.
27. Creange A, Belec L, Clair B, Raphael JC, Gherardi RK. Circulating tumor necrosis factor (TNF)-alpha and soluble TNF-alpha receptors in patients with Guillain-Barre syndrome. Journal of neuroimmunology. 1996;68(1-2):95-9.
28. Radhakrishnan VV, Sumi MG, Reuben S, Mathai A, Nair MD. Serum tumour necrosis factor-alpha and soluble tumour necrosis factor receptors levels in patients with Guillain-Barre syndrome. Acta neurologica Scandinavica. 2004;109(1):71-4.
29. Zhang HL, Hassan MY, Zheng XY, Azimullah S, Quezada HC, Amir N, et al. Attenuated EAN in TNF-alpha deficient mice is associated with an altered balance of M1/M2 macrophages. PloS one. 2012;7(5):e38157.
30. Zhang Z, Zhang ZY, Schluesener HJ. Compound A, a plant origin ligand of glucocorticoid receptors, increases regulatory T cells and M2 macrophages to attenuate experimental autoimmune neuritis with reduced side effects. Journal of immunology (Baltimore, Md : 1950). 2009;183(5):3081-91.
31. Atri C, Guerfali FZ, Laouini D. Role of Human Macrophage Polarization in Inflammation during Infectious Diseases. International journal of molecular sciences. 2018;19(6).
32. Kiefer R, Kieseier BC, Stoll G, Hartung HP. The role of macrophages in immune-mediated damage to the peripheral nervous system. Progress in neurobiology. 2001;64(2):109-27.
33. Ji W, Wang L, He S, Yan L, Li T, Wang J, et al. Effects of acute hypoxia exposure with different durations on activation of Nrf2-ARE pathway in mouse skeletal muscle. PloS one. 2018;13(12):e0208474.

34. Cuadrado A, Kugler S, Lastres-Becker I. Pharmacological targeting of GSK-3 and NRF2 provides neuroprotection in a preclinical model of tauopathy. Redox biology. 2018;14:522-34.
35. Park SY, Choi YW, Park G. Nrf2-mediated neuroprotection against oxygen-glucose deprivation/reperfusion injury by emodin via AMPK-dependent inhibition of GSK-3beta. The Journal of pharmacy and pharmacology. 2018;70(4):525-35.
36. Tannahill GM, Curtis AM, Adamik J, Palsson-McDermott EM, McGettrick AF, Goel G, et al. Succinate is an inflammatory signal that induces IL-1beta through HIF-1alpha. Nature. 2013;496(7444):238-42.
37. Hawkins KE, Joy S, Delhove JM, Kotiadis VN, Fernandez E, Fitzpatrick LM, et al. NRF2 Orchestrates the Metabolic Shift during Induced Pluripotent Stem Cell Reprogramming. Cell reports. 2016;14(8):1883-91.
38. Kim TH, Hur EG, Kang SJ, Kim JA, Thapa D, Lee YM, et al. NRF2 blockade suppresses colon tumor angiogenesis by inhibiting hypoxia-induced activation of HIF-1alpha. Cancer research. 2011;71(6):2260-75.
39. Malec V, Gottschald OR, Li S, Rose F, Seeger W, Hanze J. HIF-1 alpha signaling is augmented during intermittent hypoxia by induction of the Nrf2 pathway in NOX1-expressing adenocarcinoma A549 cells. Free radical biology & medicine. 2010;48(12):1626-35.
40. Naranjo-Suarez S, Carlson BA, Tsuji PA, Yoo MH, Gladyshev VN, Hatfield DL. HIF-independent regulation of thioredoxin reductase 1 contributes to the high levels of reactive oxygen species induced by hypoxia. PloS one. 2012;7(2):e30470.
41. Guan SP, Tee W, Ng DS, Chan TK, Peh HY, Ho WE, et al. Andrographolide protects against cigarette smoke-induced oxidative lung injury via augmentation of Nrf2 activity. British journal of pharmacology. 2013;168(7):1707-18.

Figures

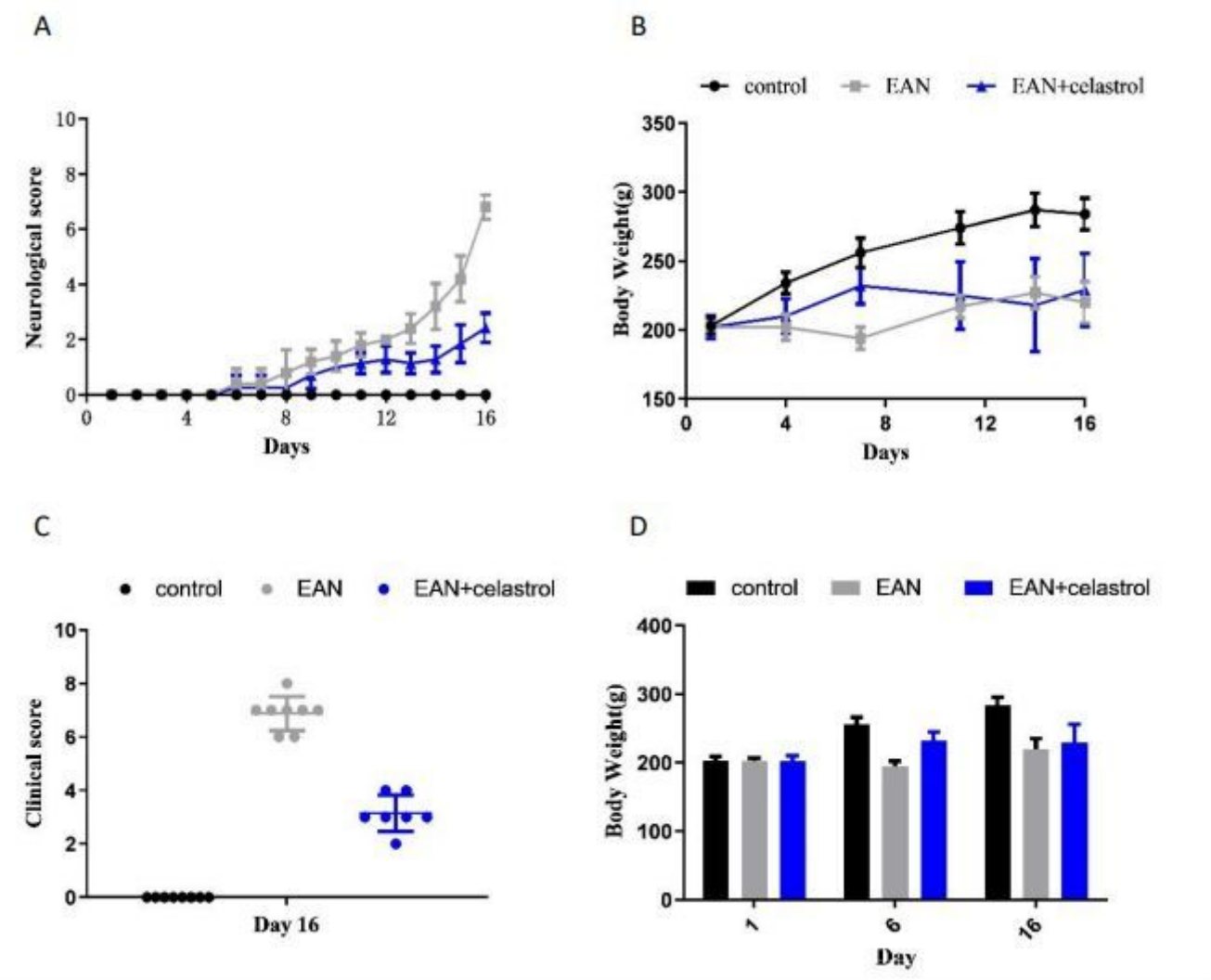

Figure 1

Celastrol ameliorates the pathogenic course of EAN. Neurological scores and weight trends were assessed in control, EAN and EAN+celastrol rats. The results are presented as the mean±SD ($P<0.05$). A. The mean neurological scores were significantly decreased in the EAN+celastrol group compared to those in the EAN group from day 8 to day 16 p.i. ($P<0.05$ for each time point). B. Compared to those of the control group, the mean body-weight trends of rats were decreased in the EAN group while this decrease occurred more slowly in the EAN+celastrol group relative to that of the EAN group. C. Compared to those in EAN rats, the mean peak neurological scores in EAN+celastrol rats were significantly decreased ($P<0.05$). D. Compared to that in the EAN group, celastrol treatment increased the body weight on day 6 and day 16 (p.i.).

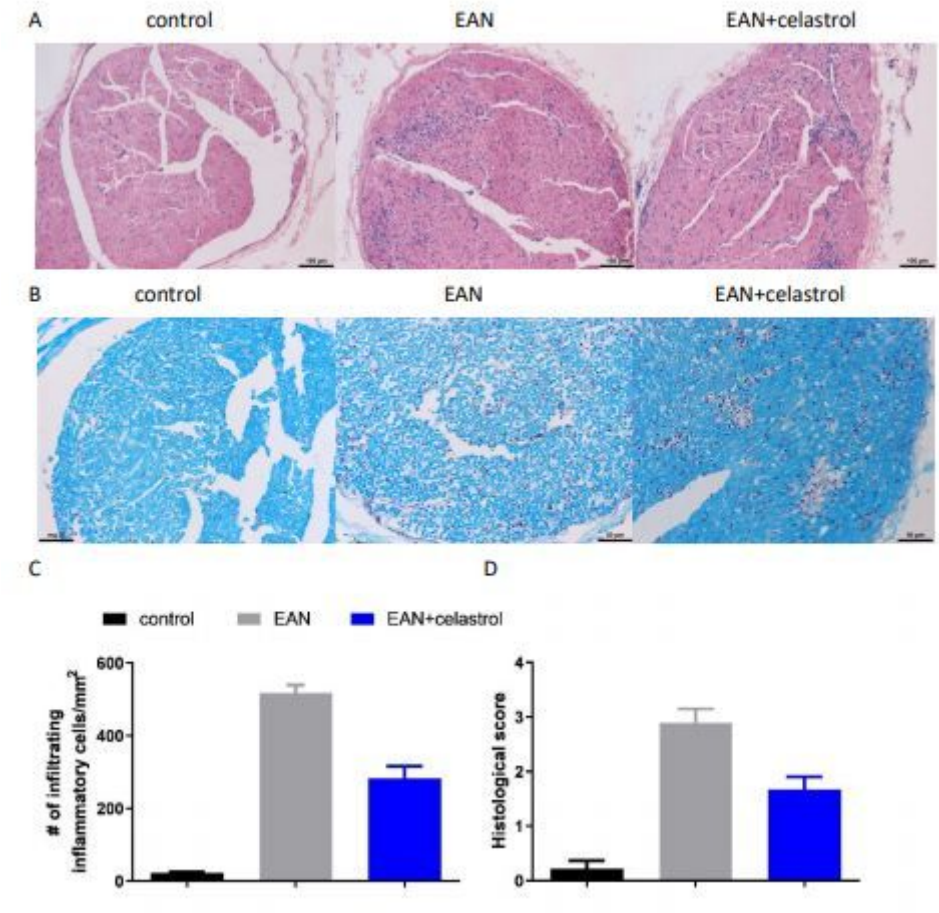

Figure 2

Celastrol treatment ameliorates demyelination and the infiltration of inflammatory cells in sciatic nerves of EAN. Representative cross-sections of sciatic nerves from control, EAN and EAN+celastrol are stained with HE (A) and LFB (B) at day 16 (p.i.). C. The number of infiltrating inflammatory cells per square millimeter was calculated as described in the methods. Compared with those in the EAN group, celastrol treatment significantly decreased the numbers of infiltrating inflammatory cells at day 16 (p.i.) ($P<0.05$). D. Histological scores were measured, as described in the methods, to evaluate the severity of demyelination according to a semiquantitative grading system. Compared with that of the EAN group, celastrol treatment significantly reduced the mean histological score at day 16 (p.i.) ($P<0.05$).

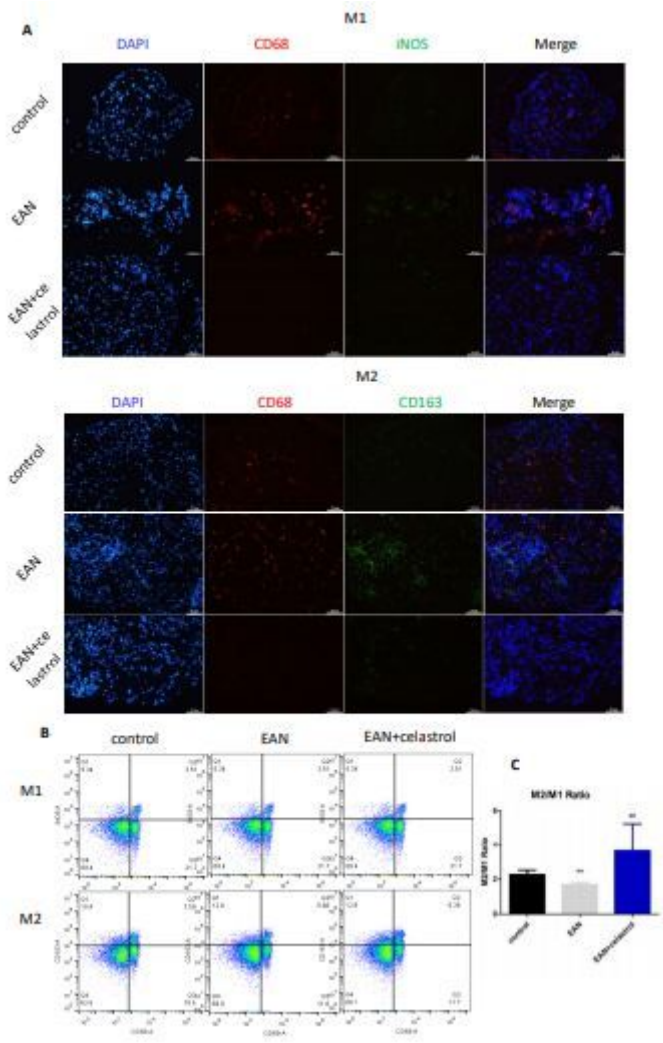

Figure 3

Celastrol promotes polarization of macrophages to the M2 phenotype in EAN. Representative cross sections of macrophage polarization in sciatic nerves from control, EAN and EAN+celastrol groups are immunofluorescently stained at day 16 (p.i.) (A). Spleen mononuclear cells were harvested for flow cytometry at day 16 (p.i.) (B). Celastrol treatment decreased the numbers of infiltrating cells in EAN ($P<0.05$) (A). Meanwhile, the M2/M1 macrophage ratio was significantly increased in the EAN+celastrol group compared to that in the EAN group ($P<0.05$). The flow cytometry results also showed the same alteration in spleen mononuclear cells (B, C), as celastrol treatment increased the M2/M1 macrophage ratio in the spleen as compared to that in the EAN group ($P<0.05$).

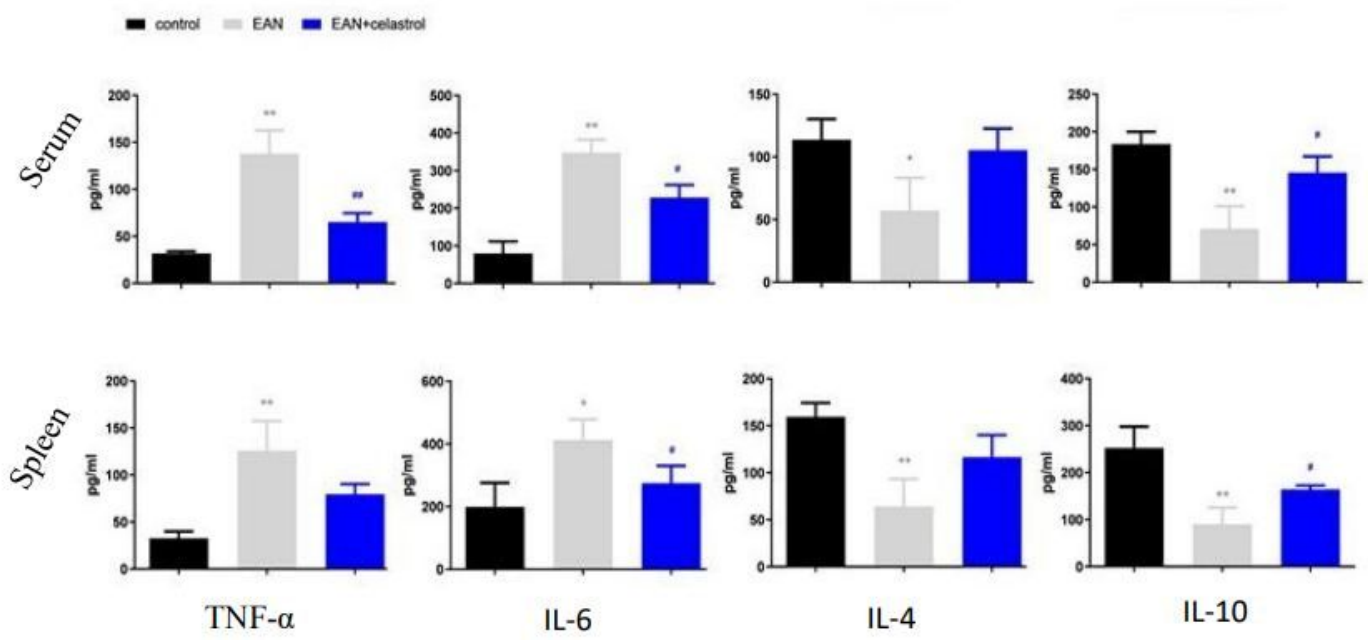

Figure 4

Celastrol reduces inflammatory cytokines while boosting anti-inflammatory cytokines in EAN. Cytokine levels were evaluated in sera and spleens by ELISAs at day 16 (p.i.). The levels of pro-inflammatory cytokines (e.g., TNF-α, IL-6) were decreased significantly in the celastrol group compared to those in the EAN group ($P<0.05$). The levels of anti-inflammatory cytokines (e.g., IL-4, IL-10) were increased significantly in the celastrol group compared to those in the EAN group ($P<0.05$).

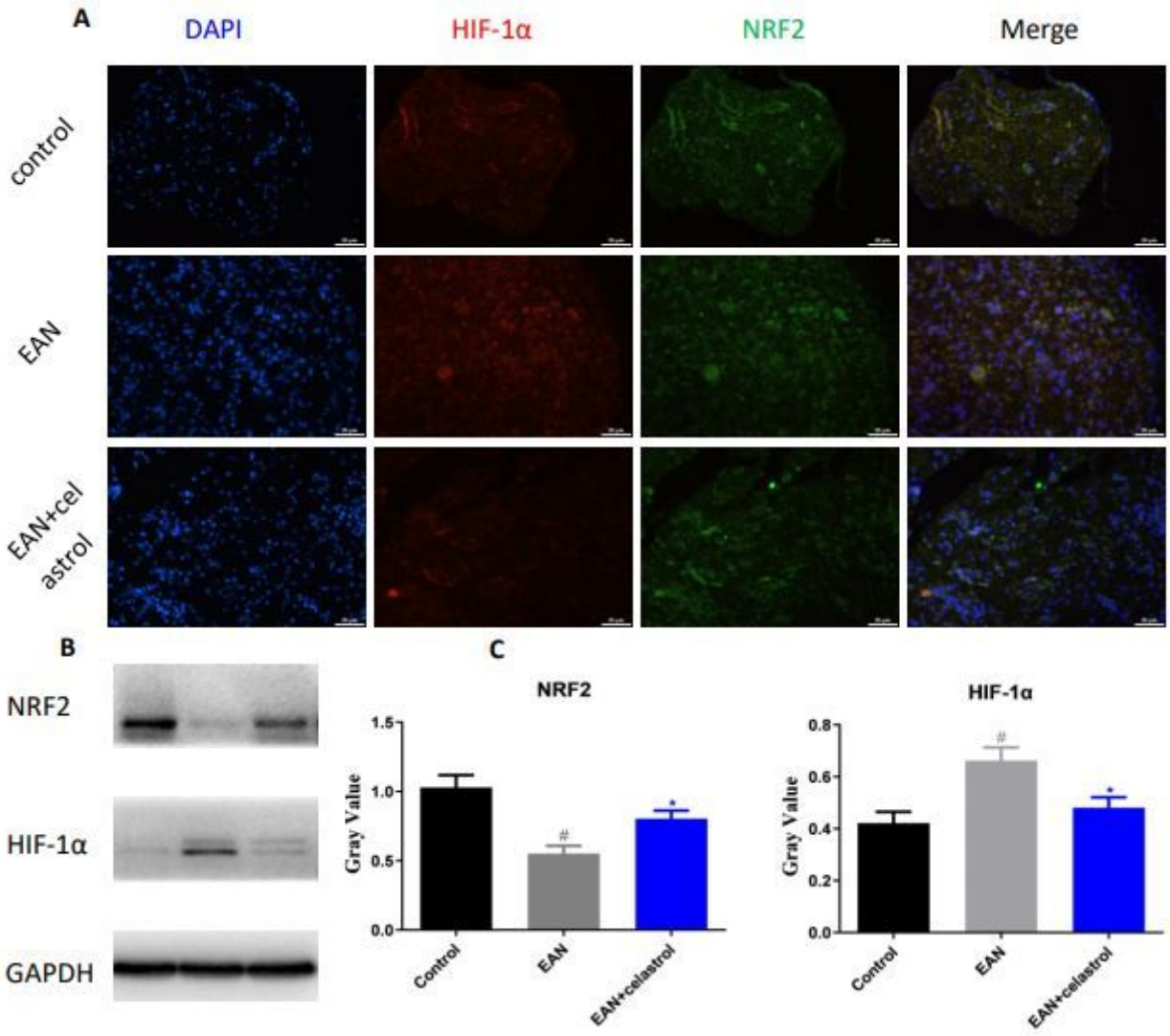

Figure 5

Celastrol regulates the NRF2/HIF-1α hypoxic pathway in EAN. Representative cross-sections of sciatic nerves from the three groups are immunofluorescently stained at day 16 (p.i.) (A). The sciatic nerves were harvested for Western blotting at day 16 (p.i.) (B). Celastrol treatment significantly upregulated the expression of NRF2 and downregulated the expression of HIF-1α in the EAN group compared to these parameters in the control group ($P<0.05$) (A). The Western-blot results showed the same change of NRF2/HIF-1α among the experimental groups (B, C). The expression of NRF2 was significantly increased while the expression of HIF-1α was decreased in the EAN+celastrol group compared to these parameters in the EAN group.

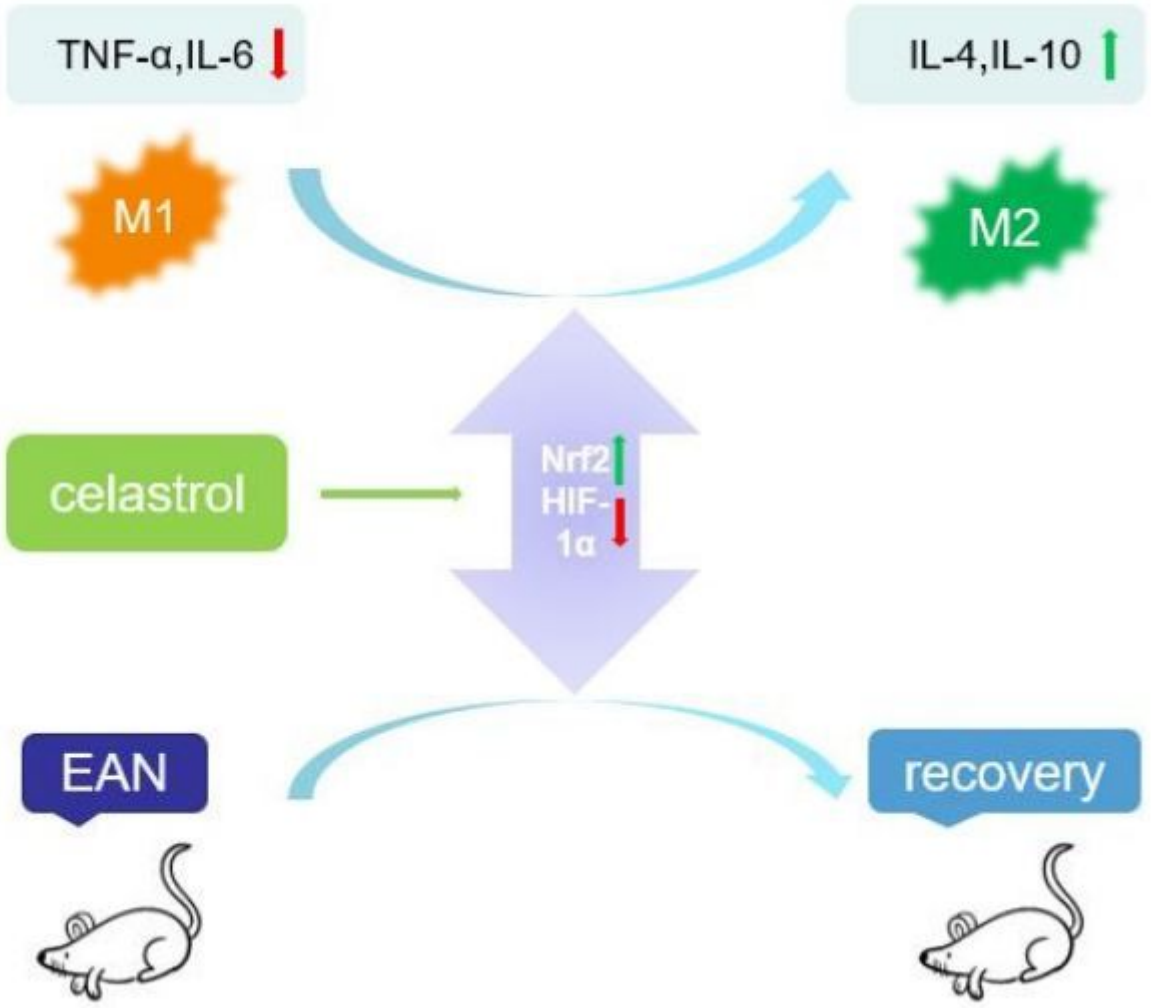

Figure 6

Effect of celastrol on EAN is mediated by altering the polarization of macrophages and the inflammatory cytokines. Macrophages play a pivotal role in neuroinflammation on EAN. Celastrol ameliorates the severity of EAN by altering the polarization of macrophages into M2. Moreover, celastrol reduces inflammatory cytokines while boosting anti-inflammatory cytokines. The mechanism underlying celastrol on macrophage polarization may be mediated by the NRF2/ HIF-1α pathway.